

Deep Recurrent Encoder: A scalable end-to-end network to model brain signals

Omar Chehab^{1,2*}, Alexandre Défossez^{1*}, Jean-Christophe Loiseau³,
Alexandre Gramfort², Jean-Remi King^{1,4†}

¹Facebook AI Research

²Université Paris-Saclay, Inria, CEA, Palaiseau, France

³ENSAM, Paris, France

⁴École normale supérieure, PSL University, CNRS, Paris, France

March 30, 2021

Abstract

Understanding how the brain responds to sensory inputs is challenging: brain recordings are partial, noisy, and high dimensional; they vary across sessions and subjects and they capture highly nonlinear dynamics. These challenges have led the community to develop a variety of preprocessing and analytical (almost exclusively linear) methods, each designed to tackle one of these issues. Instead, we propose to address these challenges through a specific end-to-end deep learning architecture, trained to predict the brain responses of multiple subjects at once. We successfully test this approach on a large cohort of magnetoencephalography (MEG) recordings acquired during a one-hour reading task. Our Deep Recurrent Encoding (DRE) architecture reliably predicts MEG responses to words with a three-fold improvement over classic linear methods. To overcome the notorious issue of interpretability of deep learning, we describe a simple variable importance analysis. When applied to DRE, this method recovers the expected evoked responses to word length and word frequency. The quantitative improvement of the present deep learning approach paves the way to better understand the nonlinear dynamics of brain activity from large datasets.

Keywords: Magnetoencephalography (MEG), Encoding, Forecasting, Reading

1 Introduction

A major goal of cognitive neuroscience consists in identifying how the brain responds to distinct experimental conditions. This objective faces three main challenges. First, we do not know *what* stimulus features the brain represents. Second, we do not know *how* such information is represented in the neuronal dynamics. Third, the available data are generally noisy, partial, high-dimensional, and variable across recording sessions (King et al., 2020b; Iturrate et al., 2014).

The first challenge – identifying the features driving brain responses – is at the heart of neuroscientific investigations. For example, it was originally unknown whether the movement, the size and/or the orientation of visual stimuli drove the firing rate of V1 neurons, until Hubel and Wiesel famously disentangled these features (Hubel and Wiesel, 1959). Similarly, it was originally unknown whether landmarks, speed or loca-

*Equal contribution

†Corresponding author jeanremi@fb.com

tion drove hippocampal responses until O’Keefe’s discovery of place cells (O’Keefe and Dostrovsky, 1971). In both of these historical cases, the features driving neuronal responses were discovered by manipulating them *experimentally* (e.g. by varying the orientation of a visual stimulus while holding its position and size). However, not only is this approach time consuming, but it can sometimes be difficult to implement. In language, for example, the length of words inversely correlates with their frequency in everyday usage (e.g. ”HOUSE” is more frequent than ”RESIDENCE”), their lexical category (e.g. NOUN, VERB etc), their position in the sentence etc. To determine whether the brain specifically responds to one or several of these features, it is thus common to use general linear model (GLM) to determine *analytically* the (combination of) features that suffices to account for brain responses (Naselaris et al., 2011).

Specifically, GLM would, here, consist in fitting a linear regression to predict a brain response to each word (e.g., the BOLD amplitude of a fMRI voxel, the voltage of an electrode, or the firing rate of a neuron) from a set of hypothetical features (e.g. word frequency, lexical category, position in the sentence etc) (Poline and Brett, 2012). The resulting regression coefficients (often referred to as β values), would indicate, under normal, homoscedasticity and linear assumptions, whether the corresponding brain response varies with each feature. As each feature needs to be explicitly specified in the analysis, GLMs can only reveal brain responses to features predetermined by the analyst (Poldrack et al., 2008). For example, a standard GLM modeling hippocampal responses and input with a POSITION parameter would not be able to reliably predict a brain response to ACCELERATION (Benjamin et al., 2018). Yet, feature identification is typically restricted to linear models, because interpreting nonlinear combination of features is non-trivial, especially with high-dimensional models (King et al., 2020b; Naselaris et al., 2011; Benjamin et al., 2018).

The second challenge to the analysis of brain signals is to reveal *how* each feature is encoded in the dynamics of neuronal responses. This challenge is particularly pregnant in the case of temporally resolved neural recordings. For example, when listening to natural sounds, the brain responses to the audio stream are highly correlated over time, making identification difficult. To handle temporal correlations in electrophysiological recordings, it is standard to employ a Temporal Receptive Field (TRF) model (Aertsen and Johannesma, 1981; Smith and Kutas, 2015a,b; Holdgraf et al., 2017; Crosse et al., 2016; Gonçalves et al., 2014; Martin et al., 2014; Lalor and Foxe, 2009; Ding and Simon, 2013; Sassenhagen, 2019) (also referred to as Finite Impulse Response (FIR) analysis in fMRI (Poline and Brett, 2012), and Distributed Lag modeling in statistics (Cromwell and Terraza, 1994)). TRF aims to predict neural responses to exogenous stimulation (or vice versa, in the case of decoding) by fitting a linear regression with a fixed time-lag window of past sensory stimuli. Contrary to event-locked (“evoked”) analyses, TRF can thus learn to disentangle temporally overlapping features and brain events.

Finally, the third challenge to the analyses of brain signals is signal-to-noise ratio. Subjects can only be recorded for a limited period. Standard practices thus generally use multiple sessions and subjects within a study, in the hope to average-out the noise across subjects. Yet, the reliability of a brain signal can be dramatically reduced because of inter-individual and, to a lesser extent, inter-session variability. In addition, important noise factors such as eye blinks, head movements, cardiac, and facial muscle activity can heavily corrupt the neural recordings. A wide variety of noise reduction methods (e.g. Vigário et al. (1998); Uusitalo and Ilmoniemi (1997); Barachant et al. (2011); Sabbagh et al. (2020)) have been developed to address these issues *analytically*. In particular, it is increasingly common to implement alignment across subjects or sessions using linear methods such as canonical correlation analysis (CCA), partial least square regression (PLS) and back-to-back regressions (B2B) (de Cheveigné et al., 2019; Xu et al., 2012; Lim et al., 2017; King et al., 2020a). These methods consist in identifying the recording dimensions that systematically covary with one-another given the same stimulus presentation, and thus naturally remove the artefactual components that are independent of the stimuli.

Overall, the methods introduced to tackle these challenges present major limitations. In particular, most of them are based on linear assumptions, which leads them to miss nonlinear dynamics such as super-additive or any interaction effects. Moreover, most of these methods model brain responses independently of its basal state. For example, neural adaptation leads brain responses to dampen if stimulations are temporally adjacent (Noguchi et al., 2004). Similarly, visual responses depend on subjects attention as well as on the alpha power of the visual cortex (Foxy and Snyder, 2011; VanRullen, 2016). GLMs and TRFs are typically only input with exogenous information from the stimuli, and therefore cannot capture interactions between initial brain states and following brain responses. Finally, TRF is inadequate to capture slow and oscillatory dynamics. This issue can be partially mitigated by increasing the receptive field of these linear models. However, changing the receptive field can dramatically increase the number of parameters. For example, slow brain oscillations can be modeled with only two variables, position and acceleration, yet a TRF would need a receptive field spanning the entire oscillation.

Here, we propose to simultaneously address these challenges with a unique end-to-end “Deep Recurrent Encoding” (DRE) neural network trained to robustly predict brain responses from both (i) past brain states and (ii) current experimental conditions. We test DRE on magneto-encephalography (MEG) recordings of human subjects during a one-hour long reading task. Such recordings indeed suffer from all of the issues detailed above (Baillet, 2017): MEG recordings are (1) extremely noisy, (2) high-dimensional (about 300 sensors sampled around 1 kHz), (3) greatly variable across individuals, (4) characterized by complex dynamics, and (5) acquired during a task involving complex stimulus features.

The paper is organized as follows. First, we introduce a common notation across the standard models of brain responses to exogeneous stimulation, motivate the introduction of each component of our DRE architecture, and describe our evaluation metrics. Second, we describe the MEG data used to test these methods. Third, we report the encoding performance and interpretation analyses obtained with each model in light of the neuroscience literature. Finally, we conclude with a critical appraisal of this work and the venues it opens.

2 Materials and Method

2.1 Problem formalization

In the case of MEG, the measured magnetic fields x reflect a tiny subset of brain dynamics h — specifically a partial and macroscopic summation of the presynaptic potentials input to pyramidal cortical cells. Given the position and precision of MEG sensors and Maxwell’s electromagnetic equations, it is standard to assume that these neuronal magnetic fields have a linear, stationary, and instantaneous relationship with the magnetic fields measured with MEG sensors (Hämäläinen et al., 1993). We refer to this “readout operator” as C , a matrix which is subject-specific because it depends on the location of pyramidal neurons in the cortex and thus on the anatomy of each subject. Furthermore, the brain dynamics governed by a function f evolve according to their past and to external stimuli u (Wilson and Cowan, 1972). In sum, we can formulate the MEG problem as follows:

$$\begin{cases} x_{\text{current}} &= C h_{\text{current}} \\ h_{\text{current}} &= f(h_{\text{past}}, u_{\text{current}}) \end{cases}$$

2.2 Operational Objective

Here, we aim to parameterize f with θ and learn θ and C to obtain a statistical (as opposed to biologically constrained as in (Friston et al., 2003)) generative model of observable brain activity that accurately predicts MEG activity $\hat{x} \in \mathbb{R}^{d_x}$ given an initial state and a series of stimuli.

Notations We denote by $u_t \in \mathbb{R}^{d_u}$ the stimulus with d_u encoded features at time t , $x_t \in \mathbb{R}^{d_x}$ the MEG recording with d_x sensors, \hat{x}_t its estimation, and by $h_t \in \mathbb{R}^{d_h}$ the underlying brain activity. Because the true underlying brain dynamics are never known, h will always refer to a model estimate. To facilitate the parametrization of f , it is common in the modeling of dynamical systems to explicitly create a "memory buffer" by concatenating successive lags. We adopt the bold notation $\mathbf{h}_{t-1:t-\tau_h} := [h_{t-1}, \dots, h_{t-\tau_h}] \in \mathbb{R}^{d_h \tau_h}$ for flattened concatenation of $\tau_h \in \mathbb{N}$ time-lagged vectors. With these notations, the dynamical models considered in this paper are described as:

$$\begin{cases} x_t &= Ch_t \\ h_t &= f_\theta(\mathbf{h}_{t-1:t-\tau_h}, \mathbf{u}_{t:t-\tau_u}) \end{cases} \quad (1)$$

where

- $f : \mathbb{R}^{d_h \tau_h + d_u (\tau_u + 1)} \rightarrow \mathbb{R}^{d_h}$ governs brain dynamics given the preceding brain states and external stimuli
- $C \in \mathbb{R}^{d_h \times d_x}$ is a linear, stationary, instantaneous and subject-specific observability operator that makes a subset of the underlying brain dynamics observable to the MEG sensors.

2.3 Models

Temporal Receptive Field (TRF) Temporal receptive fields (TRF) (Aertsen and Johannesma, 1981) is arguably the most common model for predicting neural time series in response to exogeneous stimulation. The TRF equation is that of control-driven linear dynamics:

$$h_t = f_\theta(\mathbf{h}_{t-1:t-\tau_h}, \mathbf{u}_{t:t-\tau_u}) = B\mathbf{u}_{t:t-\tau_u} , \quad (2)$$

where $B \in \mathbb{R}^{d_h \times d_u \cdot (\tau_u + 1)}$ is the convolution kernel and $\theta = \{B\}$. By definition, the TRF kernel encodes the input-output properties of the system, namely, its characteristic time scale, its memory, and thus its ability to sustain an input over time. The TRF kernel scales linearly with the duration of the neural response to the stimulus. For example, a dampened oscillation evoked by the stimulus could last one hundred time samples ($\tau_u = 99$) and would require $B \in \mathbb{R}^{d_h \times 100d_u}$ even though it is governed by three instantaneous variables (position, velocity, and acceleration). To tackle this issue of dimensionality, we introduce a recurrent component to the model.

Recurrent Temporal Receptive Field (RTRF) A Recurrent Temporal Receptive Field (RTRF) is a linear auto-regressive model. The RTRF with exogenous input can model time-series from its own past (e.g., past brain activity) *and* from exogeneous stimuli. Unrolling the recurrence reveals that current brain activity can be expressed in terms of past activity. This corresponds to recurrent dynamics with control:

$$h_t = f_\theta(\mathbf{h}_{t-1:t-\tau_h}, \mathbf{u}_{t:t-\tau_u}) = A\mathbf{h}_{t-1:t-\tau_h} + B\mathbf{u}_{t:t-\tau_u} , \quad (3)$$

where the matrix $A \in \mathbb{R}^{d_h \times (d_h \cdot \tau_h)}$ encodes the recurrent dynamics of the system and $\theta = \{A, B\}$.

The dependency of h_t on h_{t-1} in (3) means we need to unroll the expression of h_{t-1} in order to compute h_t . However, it has been shown that linear models perform poorly in this case, as terms of the form A^t (A to the power t) will appear, with either exploding or vanishing eigenvalues. This rules out optimization with first order methods due to the poor conditioning of the problem (Bottou et al., 2018), or using a closed-form solution. To circumvent unrolling the expression of h_{t-1} , we need to obtain it from what is measured at time $t - 1$. This assumes the existence of an inverse relationship from x_{t-1} to h_{t-1} , here assumed linear

based on the pseudo inverse of C : $h_{t-1} = C^\dagger x_{t-1}$. As a result, h_t and x_t are identifiable to one another and solving (3) is doable in closed form, as a regular linear system. Initializing the RTRF dynamics with the pre-stimulus data writes as:

$$h_t = C^\dagger x_t \quad \forall t \in \{0, \dots, \tau_h - 1\} , \quad (4)$$

where τ_h is chosen to match the duration pre-stimulus τ .

Though the recurrent component of the RTRF allowed to reduce the receptive field τ_u of TRF, it is nevertheless constrained to maintain a ‘sufficiently big’ receptive field τ_h to initialize over τ_h steps. The following model, DRE, will avoid this issue, and also not require that h_t and x_t are identifiable via a linear inversion.

Deep Recurrent Encoder (DRE) DRE is an architecture based on the Long-Short-Term-Memory (LSTM) computational block (Hochreiter and Schmidhuber, 1997). It is useful to think of the LSTM as a “black-box nonlinear dynamical model”, which composes the RTRF building block with nonlinearities and a memory module which reduces the need for receptive fields, so that $\tau_h = 1$ and $\tau_u = 0$. It is here employed to capture nonlinear dynamics evoked by a stimulus. A single LSTM layer writes as (Hochreiter and Schmidhuber, 1997):

$$\begin{cases} h_t &= f_\theta(\mathbf{h}_{t-1:t-\tau_h}, \mathbf{u}_{t:t-\tau_u}) = o_t \odot \tanh(m_t) \\ m_t &= d_t \odot m_{t-1} + i_t \odot \tilde{m}_t \\ \tilde{m}_t &= \tanh(Ah_{t-1} + Bu_t) \end{cases} , \quad (5)$$

where the tanh and sigmoid σ nonlinearities are applied element-wise, \odot is the Hadamard (element-wise) product, and $d_t, i_t, o_t \in (\mathbb{R}^{d_m})^3$ are data-dependent vectors with values between 0 and 1 modeled as forget (or drop), input, and output gates, respectively. The memory module $m_t \in \mathbb{R}^{d_m}$ thus interpolates between a “past term” $m_{t-1} \in \mathbb{R}^{d_m}$ and a “prediction term” $\tilde{m}_t \in \mathbb{R}^{d_m}$, taking h_t as input. The “prediction term” resembles that of the previous RTRF model except that it is here composed with a tanh nonlinearity which conveniently normalizes the signals.

Again, the dependency of h_t on h_{t-1} in (3) means we need to unroll the expression of h_{t-1} to compute h_t . While this is numerically unstable for the RTRF, the LSTM is designed so that h_t and its gradient are stable even for large values of t . As a result, h_t and x_t need not to be identifiable to one another. In other words, contrary to RTRF, the LSTM allows h_t to represent a hidden state containing potentially more information than its corresponding observation x_t .

We now motivate four modifications made to the standard LSTM.

First, we help it to recognize when (not) to sustain a signal, by augmenting the control u_t with a mask embedding $p_t \in \{0, 1\}$ indicating whether the MEG signal is provided (i.e. 1 before word onset and 0 thereafter). Second, we automatically learn to align subjects with a dedicated subject embedding layer. Indeed, a shortcoming of standard brain encoding analyses is that they are commonly performed on each subject separately. This, however, implies that one cannot exploit the possible similarities across subjects. Here, we adapt the LSTM in the spirit of Défossez et al. (2018) so that a *single* model is able to leverage information across multiple subjects by augmenting the control u_t with a “subject embedding” $s \in \mathbb{R}^{d_s}$, that is learnt for each subject. Note that this amounts to learning a matrix in $\mathbb{R}^{d_s \times n_s}$ applied to the one-hot-encoding of the subject number. Setting $d_s < n_s$, this allows to use the same LSTM block to model subject-wise variability and to train across subjects simultaneously while leveraging similarities across subjects.

Third, for comparability purposes, RTRF and LSTM should access the same (MEG) information pre-stimulus $\mathbf{x}_{\tau:1}$. Incorporating the initial MEG, before word onset, is thus done by augmenting the control with $p_t \odot x_t$. The extended control reads: $\tilde{u}_t = [u_t, s, p_t, p_t \odot x_t]$, and the LSTM with augmented control \tilde{u}_t finally reads:

$$h_t = f_\theta(\mathbf{h}_{t-1:t-\tau_h}, \tilde{\mathbf{u}}_{t:t-\tau_u}) = \text{LSTM}_\theta(h_{t-1}, \tilde{u}_t) = \text{LSTM}_\theta(\text{LSTM}_\theta(h_{t-2}, \tilde{u}_{t-1}), \tilde{u}_t) . \quad (6)$$

In practice, to maximize expressivity, two modified LSTM blocks are stacked on top of one another (Figure 1).

After introducing a nonlinear dynamical system for h_t , one can also extend the model (1) challenging the linear instantaneous mixing from h_t to x_t . Introducing two new nonlinear functions d and e , respectively parametrized by θ_2 and θ_3 , a more general model reads:

$$\begin{cases} \mathbf{x}_{t:t-\tau_x+1} & = d_{\theta_2}(h_t) \\ h_t & = f_{\theta_1}(\mathbf{h}_{t-1:t-\tau_h}, e_{\theta_3}(\tilde{\mathbf{u}}_{t:t-\tau_u})) \end{cases} , \quad (7)$$

where τ_x allows to capture a small temporal window of data around x_t , and τ_u is taken much larger than τ_x . Indeed (7) corresponds to (1) if one has $\tau_x = 1$ and $d_{\theta_2}(h_t) = Ch_t$, as well as $e_{\theta_3}(\tilde{\mathbf{u}}_{t:t-\tau_u}) = \mathbf{u}_{t:t-\tau_u}$. For the d and e functions, the DRE model uses the architecture of a 2 layers deep "convolutional autoencoder", with e formed by convolutions and d by transposed convolutions (Figure 1)¹.

In practice, we use a kernel size $K = 4$ for the convolutions. This impacts the receptive field of the network and the parameter τ_x . The equation (7) implies that the number of time samples in h and x are the same. However, a strong benefit of this extended model is to perform a reduction of the number of time steps by using a stride S larger than 1. By using a stride of 2, one reduces the temporal dimension by 2. Indeed it boils down to taking every other time sample from the output of the convolved time series. Given that the LSTM module is by nature sequential, this reduces the number of time steps and increases the speed of training and evaluation. Besides, there is evidence that LSTMs can only pass information over a limited number of time steps (Koutnik et al., 2014). In practice, we use d_h output channels for convolutional encoder.

2.4 Optimization losses

The dynamics for the above three models (TRF, RTRF, DRE) are given by different expressions of f_θ as well as the mappings between x and h via C for TRF and RTRF or c and e for DRE.

At test time, the models aim to accurately forecast MEG data from initial steps combined with subsequent stimuli. Consequently, one should train the models in the same setup. This boils down to minimizing a "multi-step-ahead" ℓ_2 prediction error:

$$\begin{cases} \text{minimize}_{\theta_1, \theta_2, \theta_3} & \sum_t \|x_t - \hat{x}_t\|_2^2 \\ \text{s.t.} & \mathbf{x}_{t:t-\tau_x+1} = d_{\theta_2}(h_t) \\ & h_t = f_{\theta_1}(\mathbf{h}_{t-1:t-\tau_h}, e_{\theta_3}(\tilde{\mathbf{u}}_{t:t-\tau_u})) \end{cases}$$

¹While "encoding" typically means outputting the MEG with respect to the neuroscience literature, we use "encoder" and "decoder" in the context of deep learning auto-encoders (Hinton and Salakhutdinov, 2006) in this paragraph.

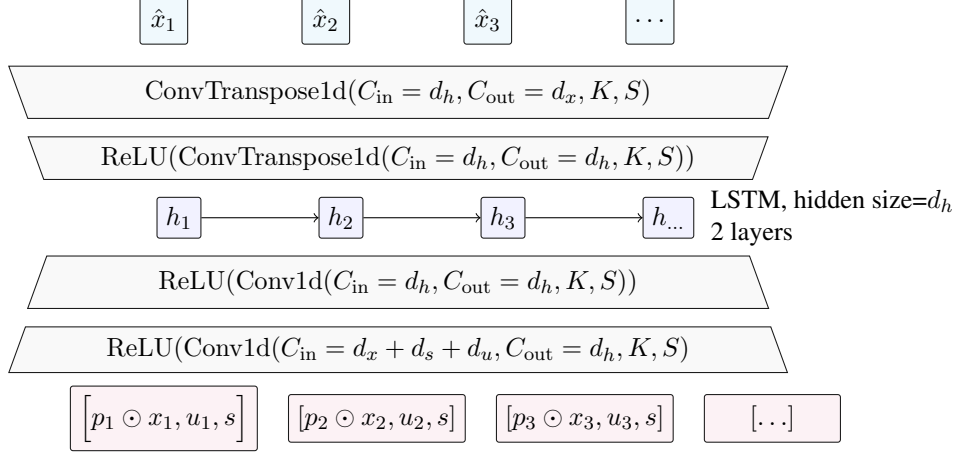


Figure 1: Representation of the Deep Recurrent Encoder (DRE) model used to predict MEG activity. The masked MEG $p_t \odot x_t$ enters the network on the bottom, along with the forcing representation u_t and the subject embedding s . The encoder transforms the input with convolutions and ReLU nonlinearities. Then the LSTM models the sequence of hidden states h_t , which are converted back to the MEG activity estimate \hat{x}_t . $\text{Conv1d}(C_{\text{in}}, C_{\text{out}}, K, S)$ represents a convolution over time with C_{in} input channels, C_{out} output channels, a kernel size K and a stride S . Similarly, $\text{ConvTransposed1d}(C_{\text{in}}, C_{\text{out}}, K, S)$ represents a transposed convolution over time.

This “multi-step-ahead” minimization requires unrolling the recurrent expression of h_t over the preceding time steps, which the LSTM-based DRE model is able to do (Bengio et al., 2015). The DRE model is input with the observed MEG at the beginning of the sequence, and must predict the future MEG measurements using the (augmented) stimulus \tilde{u}_t . Note that the mapping to and from the latent space, e_{θ_3} and d_{θ_2} , are learnt *jointly* with the dynamical operator f_{θ_1} . Furthermore, the DRE has reduced temporal receptive fields, the computational load is lightened and allows for a low or high-dimensional latent space.

For the RTRF model, as it is linear and can suffer from numerical instabilities (see above), it is trained with the “one-step-ahead” version of the predictive loss with squared ℓ_2 regularization:

$$\left\{ \begin{array}{l} \text{minimize } \theta \quad \sum_t \|x_t - \hat{x}_t\|_2^2 + \lambda \|\theta\|_2^2 \\ \text{s.t.} \quad \hat{x}_t = C h_t \\ \quad \quad h_t = f_{\theta}(\mathbf{h}_{t-1:t-\tau_h}, \mathbf{u}_{t:t-\tau_u}) \\ \quad \quad \mathbf{h}_{t-1:t-\tau_h} = C^{\dagger} \mathbf{x}_{t-1:t-\tau_h} \end{array} \right.$$

TRF models are also trained with this “one-step-ahead” loss. As mentioned above, the linear models (TRF) require a larger receptive field than the nonlinear DRE. Large receptive fields induce a computational burden, because each time lag comes with a spatial dimension of size d_h or d_u . To tackle this issue, C is chosen to reduce this spatial dimension. In practice, we choose to learn C *separately* from the dynamics to simplify the training procedure of the linear models. We do this via a Principal Component Analysis (PCA) on the averaged (evoked) MEG data. The resulting latent space will thus explain most of the variance of the original recording. Indeed, when training the TRF model on all 270 MEG sensors with no hidden state ($6.4 \pm 0.22\%$, MEAN and SEM across subjects) or using a 40-component PCA ($6.42 \pm 0.22\%$), we obtained similar performances. The pseudo-inverse C^{\dagger} required to compute the previous latent state h_{t-1} is also obtained from the PCA model. Note that dimensionality reduction via linear demixing is a standard preprocessing step in MEG (Uusitalo and Ilmoniemi, 1997; Jung et al., 2001; de Cheveigné et al., 2018).

2.5 Model Evaluation

Evaluation Method Models are evaluated using the Pearson Correlation R (between -1 and 1, here expressed as a percentage) between the model prediction \hat{x} and the true MEG signals x for each channel and each time sample (after the initial state) independently. When comparing the overall performance of the models, we average over all time steps after the stimulus onset, and over all MEG sensors for each subject independently. The reliability of prediction performance, as summarized with confidence intervals and p-values, is assessed across subjects. Similarly, model comparison is based on a non-parametric Wilcoxon rank test across subjects, that is corrected for multiple comparison using a false discovery rate (FDR) across time samples and channels.

Feature Importance To investigate what a model actually learns, we use Permutation Feature Importance (Breiman, 2001) which measures the drop in prediction performance when the j^{th} input feature u^j is shuffled:

$$\Delta R_j = R - R_j, \quad (8)$$

By tracking ΔR over time and across MEG channels, we can locate in time and space the contribution of a particular feature (e.g. word length) to the brain response.

Experiment The model weights are optimized with the training and validation sets: the penalization λ for the linear models (TRF and RTRF) is optimized with a grid search over five values distributed logarithmically between 10^{-3} and 10^3 . Training of the DRE is performed with ADAM (Kingma and Ba, 2014) using a learning rate of 10^{-4} and PyTorch’s default parameters (Paszke et al., 2019) for the running averages of the gradient and its square. The training is stopped when the error on the validation set increases. In practice, the DRE and the DRE-PCA were trained over approximately 20 and 80 epochs, respectively.

3 Experimental setup

3.1 Data

Experimental design We study a large cohort of 68 subjects from the Mother Of Unification Studies (MOUS) dataset (Schoffelen et al., 2019) who performed a one-hour reading task while being recorded with a 273-channel CTF MEG scanner. The task consisted in reading approximately 2,700 words flashed on a screen in rapid series. Words were presented sequentially in groups of 10 to 15, with a mean inter-stimulus interval of 0.78 seconds (min: 300ms, max: 1,400ms). Sequences were either random word lists or actual sentences (50% each). For this study, both conditions were used. However, this method study does not investigate the differences obtained across these two conditions. Out of the original 102 subjects, 34 were discarded from the study because we could not reliably parse their stimulus channels.

Stimulus preprocessing We focus on four well-known features associated with reading, namely word length (i.e., the number of letters in a word), word frequency in natural language (as derived by the wordfreq Python package (Speer et al., 2018), and measured on a logarithmic scale), and a binary indicator for the first and the last words of the sequence. At a given time t , each stimulus $u_t \in \mathbb{R}^4$ is therefore encoded with four values. Each feature is standardized to have zero mean and unit variance. Word length is expected to elicit an early (from $t=100$ ms) visual response in posterior MEG sensors, whereas word frequency is expected to elicit a late (from $t=400$ ms) left-lateralized response in anterior sensors. In the present task, word length and word frequency are correlated $R=-48.05\%$.

MEG Preprocessing As we are primarily interested in evoked responses (Tallon-Baudry and Bertrand, 1999), we band-pass filtered between 1 and 30 Hz and downsampled the data to 120 Hz using the MNE software (Gramfort et al., 2013b) with default settings: i.e. a FIR filter with a Hamming window, a lower transition bandwidth of 1 Hz with -6 dB attenuation at 0.50 Hz and a 7.50 Hz upper transition bandwidth with an attenuation -6 dB at 33.75 Hz.

To limit the interference of large artefacts on model training, we use Scikit-learn’s RobustScaler with default settings (Pedregosa et al., 2011) to normalize each sensor using the 25th and 75th quantiles. Following this step, most of the MEG signals will have a scale around 1. As we notice a few outliers with a larger scale, we reject any segment of 3 seconds that contains amplitudes higher than 16 in absolute value (fewer than 0.8% of the time samples).

These continuous data are then segmented between 0.5 s before and 2 s after word onset, yielding a three-dimensional MEG tensor per subject: words, sensors, and time samples relative to word onset. For each subject, we form a training, validation and test set using respectively 70%, 10% and 20% of these segments, ensuring that two segments from different sets do not originate from the same word sequence, to avoid information leakage.

3.2 Model training

Model hyper parameters We compare the three models introduced in Section 2.3. For the TRF, we use a lag on the forcing of $\tau_u = 250$ time steps (about 2 s). For the RTRF, we use $\tau_u = \tau_h = 40$ time steps. This lag corresponds to the part of the initial MEG (i.e. 333 ms out of 500 ms, at 120 Hz) that is passed to the model to predict the 2.5 s MEG sequence at evaluation time.

For the DRE model, we use a subject embedding of dimension $d_s = 16$, a latent state of dimension $d_h = 512$, a kernel size $K = 4$, and a stride $S = 2$. The subject embeddings are initialized as Gaussian vectors with zero mean and unit variance, while the weights of the convolutional layers and the LSTM are initialized using the default “Kaiming” initialization (He et al., 2015). Like its linear counterpart, the DRE is given the first 333 ms of the MEG signal to predict the complete 2.5 s of a training sample.

Ablation study To investigate the importance of the different components of the DRE model, we implement an ablation study, by fitting the model with all but one of its components. To that end, we compare the DRE to i) the DRE without using the 333 ms of pre-stimulus initial MEG data (DRE NO-INIT), ii) the DRE trained in the 40-dimensional PCA space used for the linear models (DRE PCA), iii) the DRE devoid of a subject embedding (DRE NO-SUBJECT), and to iv) the DRE devoid of the convolutional auto-encoder (DRE NO-CONV).

Code is available at <https://github.com/facebookresearch/deepmeg-recurrent-encoder>.

4 Results

We first compare three encoding models (TRF, RTRF, DRE, see methods) in their ability to accurately predict brain responses to visual words as measured with MEG. Then, we diagnose our model architecture with an ablation study over its components, to examine their relevance and pinpoint their effect on predictive performance. Finally, we interpret the models with a feature-importance analysis whose conclusions are evaluated against the neuroscience literature.

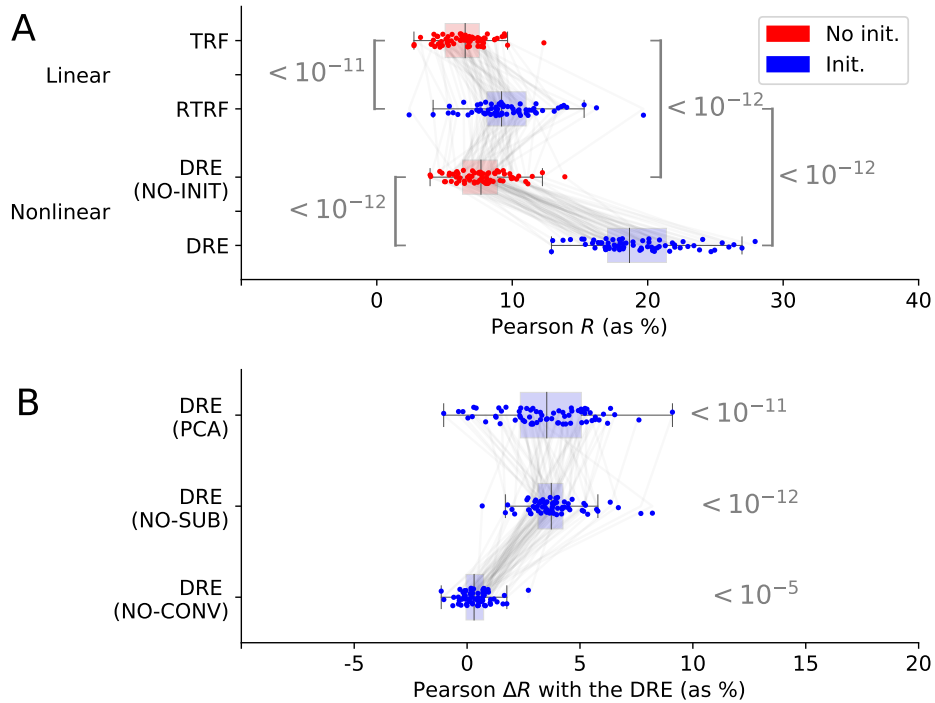


Figure 2:

A: Model Comparison. Predictive performance of different models over 68 subjects (dots) (chance=0). Boxplots indicate median and interquartile range, while gray lines follow each subject. The gray brackets indicate the p-value obtained with a pair-wise Wilcoxon comparison across subjects. Initialization and non-linearity increase predictive performance.

B: Ablation Study of our model (DRE). Pearson R mean obtained by removing a component from (Convolutional Auto-encoder or Subject-embedding) or adding an element (PCA embedding composed with the Convolutional Auto-encoder) to the DRE architecture and retraining the model, and the resulting p-values obtained by comparing the resulting scores to those of the normal DRE. Convolutions marginally impact performance of the DRE (they are essentially used for speed), but training over all MEG sensors (vs. PCA space) and using subject embeddings designed for re-alignment are responsible for an increase of approximately 4%.

Effect of nonlinearity: brain responses are better predicted with a Deep Recurrent Encoder (DRE) network than with the standard Temporal Receptive Field (TRF) We compare in Figure 2 the TRF gold standard model to our deep neural network DRE NO-INIT without initial MEG. Ignoring the MEG data in the input of the DRE model allows for a fair comparison. One can observe that the DRE NO-INIT consistently outperforms the TRF (mean correlation score $R=7.77\%$, standard error of the mean across subjects: $\pm 0.24\%$ for DRE NO-INIT vs. $6.42 \pm 0.22\%$ for TRF). This difference is strongly significant ($p < 10^{-12}$) a Wilcoxon test across subjects. A similar observation holds for the models that make use of the initial (pre-stimulus) MEG activity: the DRE ($19.38 \pm 0.41\%$) significantly ($p < 10^{-12}$) outperforms its linear counterpart, the RTRF ($9.58 \pm 0.33\%$). The 512-dimensional latent space of the DRE may have

an unfair advantage over the RTRF’s 40-dimensional Principal Components. However, even when the DRE is trained with the *same* PCA as the linear models, it maintains a higher performance ($15.85 \pm 0.45\%$, $p < 10^{-11}$). This result suggests that DRE’s performance is best attributed to its ability to capture nonlinear dynamics.

Effect of initialization with pre-stimulus MEG: brain responses depend on the initial state of the brain

Following electrophysiological findings (VanRullen, 2016; Haegens and Golumbic, 2018), we hypothesized that brain responses to sensory input may vary as a function of the state in which the brain is prior to the stimulus. Recurrent models (RTRF, DRE) are best suited for this issue: initialized with 333 ms of pre-stimulus MEG, they can use initial brain activity to predict the post-stimulus MEG. Among the linear models, the TRF is outperformed by its recurrent counterpart, the RTRF ($9.58 \pm 0.33\%$, $p < 10^{-11}$), with an average performance increment of 3.16%. The DRE ($19.38 \pm 0.41\%$) outperforms its NO-INIT counterpart ($7.77 \pm 0.24\%$, $p < 10^{-12}$), with an average performance increment of 11.61%. Indeed, the performance increase that comes with initialization is even more significant ($p < 10^{-12}$) for our nonlinear model. Together, these results suggest that brain responses to visual words depend on the on-going dynamics of brain activity prior to word onset.

Subject embeddings and hierarchical convolutions help training

To what extent are the modules added to the original LSTM relevant? To tackle this issue, we performed ablation analyses by retraining the DRE without specific components. The corresponding results are reported in panel B of Figure 2. Removing the convolutional layers led to a small but significant drop in the Pearson correlation as compared to DRE: the DRE NO-CONV’s correlation scores across subjects ($19.00 \pm 0.42\%$) are slightly lower than those obtained with DRE ($19.38 \pm 0.41\%$, $p < 10^{-5}$). In addition, convolutions multiplied the training speed on an NVIDIA V100 GPU by a factor of 1.8, from 2.6 hours for the DRE (NO-CONV) to 1.4 hours for the DRE. In sum, the convolutions may not give major advantages in terms of performance but facilitates the training.

Second, we trained the DRE devoid of the subject embedding (DRE NO-SUBJECT). This ablation induced an important drop in performance ($15.53 \pm 0.39\%$, $p < 10^{-12}$). This result validates a key part of the DRE’s architecture: the subject embedding efficiently *re-aligns* subjects’ brain responses, so that the LSTM modules can model the *shared* dynamics between subjects.

Feature importance confirms that early visual and late frontal responses are modulated by word length and word frequency, respectively

Interpreting nonlinear and/or high-dimensional models is notoriously challenging (Lipton, 2018). This issue poses a major limit to the use of deep learning of neural recordings, where interpretability remains a major goal (King et al., 2020b; Ivanova et al., 2020). While DRE faces the same types of issues as any deep neural networks, we show below that a simple feature importance analysis of the predictions of this model (as opposed to on its parameters), yields results consistent both with those obtained with linear models and with those described in the neuroscientific literature (cf. Section 2.5).

Feature importance quantifies the loss of prediction performance ΔR obtained when a unique feature is shuffled across words as compared to a non-shuffled prediction. Here, we focus our analysis on word length and word frequency, as these two features have been repeatedly associated in the literature with early sensory neural responses in the visual cortex and late lexical neural responses in the temporal cortex, respectively Figure 3 (Federmeier and Kutas, 1999; Fedorenko et al., 2016). As expected, the feature importance for word length peaked around 150 ms in posterior MEG channels, whereas the feature importance of word frequency peaked around 400 ms in fronto-temporal MEG channels, for both the TRF and the DRE mod-

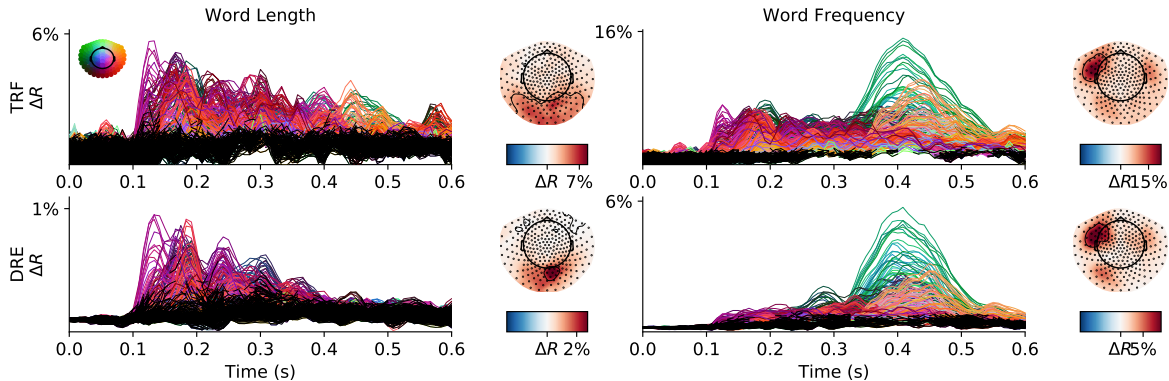


Figure 3: Permutation importance (ΔR) of word length (left column) and word frequency (right column), as a function of spatial location (color-coded by channel position, see top-left rainbow topography) and time relative to word onset for the two main encoding models (rows). The amplitudes of each line represent the mean across words and subjects for each channel. An FDR-corrected Wilcoxon test across subjects assesses the significance for each channel and time samples independently. Non-significant effects (p -value higher than 5%) are displayed in black. Overall, this feature importance analysis confirms that early visual and late frontal responses are modulated by word length and word frequency, respectively, as expected.

els. Furthermore, we recover a second phenomenon known in the literature: the *lateralization* of lexical processing in the brain. Indeed, Figure 3 shows, for the word frequency, an effect similar in shape across hemispheres, but significantly higher in amplitude for the left hemisphere (e.g. $p < 10^{-7}$ in the frontal region, $p < 10^{-8}$ in the temporal region, for the DRE).

These results suggest that, in spite of being a high dimensional and nonlinear, DRE can, in the present context, be (at least partially) interpreted similarly to linear models.

5 Discussion

The present study demonstrates that a recurrent neural network can considerably outperform several of its linear counterparts to predict neural time series. This improvement appears to be driven by three factors: (i) the ability to capture nonlinear dynamics, (ii) the ability to combine multiple subjects, and (iii) the ability to modulate predictions based on both the external stimuli and the initial state of the brain.

The gain in prediction performance does not necessarily come at the price of interpretability. Indeed, the DRE can be easily probed to reveal *which* brain regions respond *when* to the size of visual words and to their frequency in natural language (Federmeier and Kutas, 1999). In future work, this simple, univariate analysis could be extended, for example, by probing stimulus features that code for richer grammatical or lexical qualities and whose processing by the brain remains elusive. Furthermore, interaction effects between stimulus features (e.g. between a noun and a verb) or between a feature and the initial brain activity, could be explored within the same framework (Bernal et al., 2013; VanRullen, 2016).

So far, deep neural networks have not emerged as the go-to method for neuroimaging (He et al., 2020; Roy et al., 2019). This issue likely results from a combinations of factors including (i) low signal-to-noise ratio (ii) small datasets and (iii) a lack of high temporal resolution, where nonlinear dynamics may be the most prominent. Nonetheless, several studies have successfully used deep learning architectures to model brain signals (Richards et al., 2019; Güçlü and van Gerven, 2015; Kuzovkin et al., 2018). In

particular, deep nets trained on natural images, sounds or text, are being increasingly used as an *encoding* model for predicting neural responses to sensory stimulation (Yamins and DiCarlo, 2016; Kriegeskorte and Golan, 2019; Eickenberg et al., 2017; Keshishian et al., 2020). Conversely, deep nets have also been trained to *decode* sensory-motor signals from neural activity, successfully reconstructing text (Sun et al., 2020) from Electrocorticography (ECoG) recordings or images (Güçlütürk et al., 2017) from Functional magnetic resonance imaging (fMRI).

Related to the present work, Keshishian et al. (2020) compared the predictive performance of the TRF model with a nonlinear counterpart (convolutional neural network). They noted an improvement with the convolutional network, which they inspect via the receptive fields of the convolutions. This nonlinear model however did not incorporate recurrence, which has here proved useful. Similarly, Benjamin et al. (2018) showed that a recurrent neural network (LSTM) outperforms a Generalized Linear Model (GLM) analogous to the present TRF, at predicting the rate of spiking activity in a variety of motor and navigation tasks. Their LSTM architecture is similar to the present DRE devoid of (i) initialization, (ii) subject embedding and (iii) convolutional layers. Our work also involves a large dataset of 68 MEG recordings.

It is worth noting that the losses used to train the models in this paper are mean squared errors evaluated in the time domain. Therefore, the TRF, RTRF and DRE are solely trained and evaluated on their ability to predict the *amplitude* of the neural signal *at each time sample*. Consequently, the objective solely focuses on “evoked” activity, i.e. neural signals that are strictly phase-locked to stimulus onset or to previous brain signals (Tallon-Baudry and Bertrand, 1999). On the contrary, “induced” activity, e.g. changes in the amplitude of neural oscillations with a non-deterministic phase, cannot be captured by any of these models. A fundamentally distinct loss would be necessary to capture such non phase-locked neural dynamics.

As for many other scientific disciplines, deep neural networks will undoubtedly complement – if not shift – the myriad of analytical pipelines developed over the years toward standardized end-to-end modeling. While such methodological development may improve our ability to predict how the brain responds to various exogenous stimuli, the present attempt already highlights the many challenges that this approach entails.

Acknowledgements

Experiments on MEG data were made possible thanks to MNE (Gramfort et al., 2013a,b), as well as the scientific Python ecosystem: Matplotlib (Hunter, 2007), Scikit-learn (Pedregosa et al., 2011), Numpy (Harris et al., 2020), Scipy (Virtanen et al., 2020) and PyTorch (Paszke et al., 2019).

This work was supported by the French ANR-20-CHIA-0016 and the European Research Council Starting Grant SLAB ERC-YStG-676943 to AG, and by the French ANR-17-EURE-0017 and the Fyssen Foundation to JRK for his work at PSL.

Conflict of interest

The authors declare no conflict of interest.

References

A. M. H. J. Aertsen and P. I. M. Johannesma. The spectro-temporal receptive field. *Biological Cybernetics*, 42(2):133–143, Nov 1981.

- Sylvain Baillet. Magnetoencephalography for brain electrophysiology and imaging. *Nature Neuroscience*, 20(3):327–339, 2017.
- Alexandre Barachant, Stéphane Bonnet, Marco Congedo, and Christian Jutten. Multiclass brain–computer interface classification by riemannian geometry. *IEEE Transactions on Biomedical Engineering*, 59(4): 920–928, 2011.
- Samy Bengio, Oriol Vinyals, Navdeep Jaitly, and Noam Shazeer. Scheduled sampling for sequence prediction with recurrent neural networks. In C. Cortes, N. Lawrence, D. Lee, M. Sugiyama, and R. Garnett, editors, *Advances in Neural Information Processing Systems*, volume 28, pages 1171–1179. Curran Associates, Inc., 2015.
- Ari S. Benjamin, Hugo L. Fernandes, Tucker Tomlinson, Pavan Ramkumar, Chris VerSteeg, Raed H. Chowdhury, Lee E. Miller, and Konrad P. Kording. Modern machine learning as a benchmark for fitting neural responses. *Frontiers in Computational Neuroscience*, 12:56, 2018.
- Byron Bernal, Magno Guillen, and Juan Marquez. The spinning dancer illusion and spontaneous brain fluctuations: An fMRI study. *Neurocase*, 20, 08 2013.
- Léon Bottou, Frank E Curtis, and Jorge Nocedal. Optimization methods for large-scale machine learning. *Siam Review*, 60(2):223–311, 2018.
- Leo Breiman. Random forests. *Machine Learning*, 45(1):5–32, Oct 2001.
- Jeff B Cromwell and Michel Terraza. *Multivariate tests for time series models*. Sage, 1994.
- Michael J. Crosse, Giovanni M. Di Liberto, Adam Bednar, and Edmund C. Lalor. The multivariate temporal response function (mTRF) toolbox: A matlab toolbox for relating neural signals to continuous stimuli. *Frontiers in Human Neuroscience*, 10:604, 2016.
- Alain de Cheveigné, Daniel DE Wong, Giovanni M Di Liberto, Jens Hjortkjaer, Malcolm Slaney, and Edmund Lalor. Decoding the auditory brain with canonical component analysis. *NeuroImage*, 172:206–216, 2018.
- Alain de Cheveigné, Giovanni M Di Liberto, Dorothée Arzounian, Daniel DE Wong, Jens Hjortkjær, Søren Fuglsang, and Lucas C Parra. Multiway canonical correlation analysis of brain data. *NeuroImage*, 186: 728–740, 2019.
- Alexandre Défossez, Neil Zeghidour, Nicolas Usunier, Leon Bottou, and Francis Bach. Sing: Symbol-to-instrument neural generator. In S. Bengio, H. Wallach, H. Larochelle, K. Grauman, N. Cesa-Bianchi, and R. Garnett, editors, *Advances in Neural Information Processing Systems 31*, pages 9041–9051. Curran Associates, Inc., 2018.
- Nai Ding and Jonathan Z. Simon. Adaptive temporal encoding leads to a background-insensitive cortical representation of speech. *Journal of Neuroscience*, 33(13):5728–5735, 2013.
- Michael Eickenberg, Alexandre Gramfort, Gaël Varoquaux, and Bertrand Thirion. Seeing it all: Convolutional network layers map the function of the human visual system. *NeuroImage*, 152:184–194, 2017.
- Kara D. Federmeier and Marta Kutas. A rose by any other name: Long-term memory structure and sentence processing. *Journal of Memory and Language*, 41(4):469–495, 11 1999.

- Evelina Fedorenko, Terri L Scott, Peter Brunner, William G Coon, Brianna Pritchett, Gerwin Schalk, and Nancy Kanwisher. Neural correlate of the construction of sentence meaning. *Proceedings of the National Academy of Sciences*, 113(41):E6256–E6262, 2016.
- John Foxe and Adam Snyder. The role of alpha-band brain oscillations as a sensory suppression mechanism during selective attention. *Frontiers in Psychology*, 2:154, 2011.
- K J Friston, L Harrison, and W Penny. Dynamic causal modelling. *Neuroimage*, 19(4):1273–1302, 2003.
- Nuno R. Gonçalves, Robert Whelan, John J. Foxe, and Edmund C. Lalor. Towards obtaining spatiotemporally precise responses to continuous sensory stimuli in humans: A general linear modeling approach to EEG. *NeuroImage*, 97:196 – 205, 2014.
- Alexandre Gramfort, Martin Luessi, Eric Larson, Denis Engemann, Daniel Strohmeier, Christian Brodbeck, Lauri Parkkonen, and Matti Hämäläinen. MNE software for processing MEG and EEG data. *NeuroImage*, 86, 10 2013a.
- Alexandre Gramfort, Martin Luessi, Eric Larson, Denis A Engemann, Daniel Strohmeier, Christian Brodbeck, Roman Goj, Mainak Jas, Teon Brooks, Lauri Parkkonen, et al. MEG and EEG data analysis with MNE-Python. *Frontiers in neuroscience*, 7:267, 2013b.
- Yağmur Güçlütürk, Umut Güçlü, Katja Seeliger, Sander Bosch, Rob van Lier, and Marcel van Gerven. Deep adversarial neural decoding. arXiv Preprint 1705.07109, 2017.
- Umut Güçlü and Marcel van Gerven. Deep neural networks reveal a gradient in the complexity of neural representations across the ventral stream. *The Journal of Neuroscience : The Official Journal of the Society for Neuroscience*, 35:10005–10014, 07 2015.
- Saskia Haegens and Elana Zion Golumbic. Rhythmic facilitation of sensory processing: A critical review. *Neuroscience & Biobehavioral Reviews*, 86:150–165, 2018.
- Matti Hämäläinen, Riitta Hari, Risto J Ilmoniemi, Jukka Knutila, and Olli V Lounasmaa. Magnetoencephalography—theory, instrumentation, and applications to noninvasive studies of the working human brain. *Reviews of modern Physics*, 65(2):413, 1993.
- Charles R. Harris, K. Jarrod Millman, St’efan J. van der Walt, Ralf Gommers, Pauli Virtanen, David Cournapeau, Eric Wieser, Julian Taylor, Sebastian Berg, Nathaniel J. Smith, Robert Kern, Matti Picus, Stephan Hoyer, Marten H. van Kerkwijk, Matthew Brett, Allan Haldane, Jaime Fern’andez del R’io, Mark Wiebe, Pearu Peterson, Pierre G’erard-Marchant, Kevin Sheppard, Tyler Reddy, Warren Weckesser, Hameer Abbasi, Christoph Gohlke, and Travis E. Oliphant. Array programming with NumPy. *Nature*, 585(7825):357–362, September 2020. doi: 10.1038/s41586-020-2649-2. URL <https://doi.org/10.1038/s41586-020-2649-2>.
- Kaiming He, X. Zhang, Shaoqing Ren, and Jian Sun. Delving deep into rectifiers: Surpassing human-level performance on imagenet classification. *2015 IEEE International Conference on Computer Vision (ICCV)*, pages 1026–1034, 2015.
- Tong He, Ru Kong, Avram J Holmes, Minh Nguyen, Mert R Sabuncu, Simon B Eickhoff, Danilo Bzdok, Jiashi Feng, and BT Thomas Yeo. Deep neural networks and kernel regression achieve comparable accuracies for functional connectivity prediction of behavior and demographics. *NeuroImage*, 206:116276, 2020.

- Geoffrey E Hinton and Ruslan R Salakhutdinov. Reducing the dimensionality of data with neural networks. *Science*, 313(5786):504–507, 2006.
- Sepp Hochreiter and Jürgen Schmidhuber. Long short-term memory. *Neural computation*, 9(8):1735–1780, 1997.
- Christopher R. Holdgraf, Jochem W. Rieger, Cristiano Micheli, Stephanie Martin, Robert T. Knight, and Frederic E. Theunissen. Encoding and decoding models in cognitive electrophysiology. *Frontiers in Systems Neuroscience*, 11:61, 2017.
- David H Hubel and Torsten N Wiesel. Receptive fields of single neurones in the cat’s striate cortex. *The Journal of Physiology*, 148(3):574–591, 1959.
- John D Hunter. Matplotlib: A 2d graphics environment. *Computing in science & engineering*, 9(3):90–95, 2007.
- Iñaki Iturrate, Ricardo Chavarriaga, Luis Montesano, Javier Minguez, and JdR Millán. Latency correction of event-related potentials between different experimental protocols. *Journal of neural engineering*, 11(3):036005, 2014.
- Anna Ivanova, Martin Schrimpf, Leyla Isik, Stefano Anzellotti, Noga Zaslavsky, and Evelina Fedorenko. Is it that simple? the use of linear models in cognitive neuroscience. Workshop Proposal, 2020.
- T. P. Jung, S. Makeig, M. J. McKeown, A. J. Bell, T. W. Lee, and T. J. Sejnowski. Imaging brain dynamics using independent component analysis. *Proceedings of the IEEE*, 89(7):1107–1122, 2001.
- Menoua Keshishian, Hassan Akbari, Bahar Khalighinejad, Jose L Herrero, Ashesh D Mehta, and Nima Mesgarani. Estimating and interpreting nonlinear receptive field of sensory neural responses with deep neural network models. *eLife*, 9:e53445, jun 2020. ISSN 2050-084X.
- Jean-Rémi King, François Charton, David Lopez-Paz, and Maxime Oquab. Back-to-back regression: Disentangling the influence of correlated factors from multivariate observations. *NeuroImage*, 220:117028, 2020a.
- Jean-Rémi King, Laura Gwilliams, Chris Holdgraf, Jona Sassenhagen, Alexandre Barachant, Denis Engemann, Eric Larson, and Alexandre Gramfort. Encoding and decoding frameworks to uncover the algorithms of cognition. In Gazzaniga M. S. Poeppel D., Mangun G. R., editor, *The Cognitive Neurosciences*. MIT Press, 2020b.
- Diederik Kingma and Jimmy Ba. Adam: A method for stochastic optimization. *International Conference on Learning Representations*, 12 2014.
- Jan Koutnik, Klaus Greff, Faustino Gomez, and Juergen Schmidhuber. A clockwork rnn. In Eric P. Xing and Tony Jebara, editors, *Proceedings of the 31st International Conference on Machine Learning*, volume 32 of *Proceedings of Machine Learning Research*, pages 1863–1871, Beijing, China, 22–24 Jun 2014. PMLR.
- Nikolaus Kriegeskorte and Tal Golan. Neural network models and deep learning. *Current Biology*, 29(7):R231–R236, 2019.
- Ilya Kuzovkin, Raul Vicente, Mathilde Petton, Jean-Philippe Lachaux, Monica Baciú, Philippe Kahane, Sylvain Rheims, Juan Vidal, and Jaan Aru. Activations of deep convolutional neural networks are aligned with gamma band activity of human visual cortex. *Communications Biology*, 1, 12 2018.

- Edmund Lalor and John Foxe. Neural responses to uninterrupted natural speech can be extracted with precise temporal resolution. *European Journal of Neuroscience*, 31(1):189–193, 2009.
- Michael Lim, Justin Ales, Benoit Cottureau, Trevor Hastie, and Anthony Norcia. Sparse EEG/MEG source estimation via a group lasso. *PLOS ONE*, 12:e0176835, 06 2017.
- Zachary C Lipton. The mythos of model interpretability. *Queue*, 16(3):31–57, 2018.
- Stéphanie Martin, Peter Brunner, Chris Holdgraf, Hans-Jochen Heinze, Nathan E. Crone, Jochem Rieger, Gerwin Schalk, Robert T. Knight, and Brian N. Pasley. Decoding spectrotemporal features of overt and covert speech from the human cortex. *Frontiers in Neuroengineering*, 7:14, 2014.
- Thomas Naselaris, Kendrick N Kay, Shinji Nishimoto, and Jack L Gallant. Encoding and decoding in fMRI. *Neuroimage*, 56(2):400–410, 2011.
- Yasuki Noguchi, Koji Inui, and Ryusuke Kakigi. Temporal dynamics of neural adaptation effect in the human visual ventral stream. *Journal of Neuroscience*, 24(28):6283–6290, 2004. ISSN 0270-6474.
- John O’Keefe and Jonathan Dostrovsky. The hippocampus as a spatial map: Preliminary evidence from unit activity in the freely-moving rat. *Brain research*, 1971.
- Adam Paszke, Sam Gross, Francisco Massa, Adam Lerer, James Bradbury, Gregory Chanan, Trevor Killeen, Zeming Lin, Natalia Gimelshein, Luca Antiga, Alban Desmaison, Andreas Kopf, Edward Yang, Zachary DeVito, Martin Raison, Alykhan Tejani, Sasank Chilamkurthy, Benoit Steiner, Lu Fang, Junjie Bai, and Soumith Chintala. Pytorch: An imperative style, high-performance deep learning library. In H. Wallach, H. Larochelle, A. Beygelzimer, F. d’Alché Buc, E. Fox, and R. Garnett, editors, *Advances in Neural Information Processing Systems 32*, pages 8024–8035. Curran Associates, Inc., 2019.
- F. Pedregosa, G. Varoquaux, A. Gramfort, V. Michel, B. Thirion, O. Grisel, M. Blondel, P. Prettenhofer, R. Weiss, V. Dubourg, J. Vanderplas, A. Passos, D. Cournapeau, M. Brucher, M. Perrot, and E. Duchesnay. Scikit-learn: Machine Learning in Python . *Journal of Machine Learning Research*, 12:2825–2830, 2011.
- Russell A Poldrack, Paul C Fletcher, Richard N Henson, Keith J Worsley, Matthew Brett, and Thomas E Nichols. Guidelines for reporting an fMRI study. *Neuroimage*, 40(2):409–414, 2008.
- Jean-Baptiste Poline and Matthew Brett. The general linear model and fMRI: Does love last forever? *NeuroImage*, 62(2):871 – 880, 2012.
- Blake A Richards, Timothy P Lillicrap, Philippe Beaudoin, Yoshua Bengio, Rafal Bogacz, Amelia Christensen, Claudia Clopath, Rui Ponte Costa, Archy de Berker, Surya Ganguli, et al. A deep learning framework for neuroscience. *Nature Neuroscience*, 22(11):1761–1770, 2019.
- Y. Roy, H. Banville, I. Albuquerque, A. Gramfort, T.H. Falk, and J. Faubert. Deep learning-based electroencephalography analysis: a systematic review. *Journal of neural engineering*, 16(5):051001, 2019.
- David Sabbagh, Pierre Ablin, Gaël Varoquaux, Alexandre Gramfort, and Denis A. Engemann. Predictive regression modeling with MEG/EEG: from source power to signals and cognitive states. *NeuroImage*, 222:116893, 2020.
- Jona Sassenhagen. How to analyse electrophysiological responses to naturalistic language with time-resolved multiple regression. *Language, Cognition and Neuroscience*, 34(4):474–490, 2019.
- Jan-Mathijs Schoffelen, Robert Oostenveld, Nietzsche Lam, Julia Udden, Annika Hulten, and Peter Hagoort. A 204-subject multimodal neuroimaging dataset to study language processing. *Scientific Data*, 6, 12 2019.

- N.J. Smith and M. Kutas. Regression-based estimation of ERP waveforms: I. the rERP framework. *Psychophysiology*, 52(2):157–168, 2015a.
- N.J. Smith and M. Kutas. Regression-based estimation of ERP waveforms: II. nonlinear effects, overlap correction, and practical considerations. *Psychophysiology*, 52(2):169–181, 2015b.
- Robyn Speer, Joshua Chin, Andrew Lin, Sara Jewett, and Lance Nathan. Luminosinsight/wordfreq: v2.2. <https://github.com/LuminosoInsight/wordfreq>, October 2018.
- P. Sun, G. K. Anumanchipalli, and E. Chang. Brain2char: A deep architecture for decoding text from brain recordings. *Journal of Neural Engineering*, 2020.
- Catherine Tallon-Baudry and Olivier Bertrand. Oscillatory gamma activity in humans and its role in object representation. *Trends in Cognitive Sciences*, 3(4):151–162, 1999.
- Mikko Uusitalo and Risto Ilmoniemi. Signal-space projection method for separating MEG or EEG into components. *Medical and biological engineering and computing*, 35(2):135–40, 04 1997.
- Rufin VanRullen. Perceptual cycles. *Trends in cognitive sciences*, 20(10):723–735, 2016.
- Ricardo Vigário, Veikko Jousmäki, Matti Hämäläinen, Riitta Hari, and Erkki Oja. Independent component analysis for identification of artifacts in magnetoencephalographic recordings. In M. Jordan, M. Kearns, and S. Solla, editors, *Advances in Neural Information Processing Systems*, volume 10, pages 229–235. MIT Press, 1998.
- Pauli Virtanen, Ralf Gommers, Travis E. Oliphant, Matt Haberland, Tyler Reddy, David Cournapeau, Evgeni Burovski, Pearu Peterson, Warren Weckesser, Jonathan Bright, Stéfan J. van der Walt, Matthew Brett, Joshua Wilson, K. Jarrod Millman, Nikolay Mayorov, Andrew R. J. Nelson, Eric Jones, Robert Kern, Eric Larson, C J Carey, İlhan Polat, Yu Feng, Eric W. Moore, Jake VanderPlas, Denis Laxalde, Josef Perktold, Robert Cimrman, Ian Henriksen, E. A. Quintero, Charles R. Harris, Anne M. Archibald, Antônio H. Ribeiro, Fabian Pedregosa, Paul van Mulbregt, and SciPy 1.0 Contributors. SciPy 1.0: Fundamental Algorithms for Scientific Computing in Python. *Nature Methods*, 17:261–272, 2020. doi: 10.1038/s41592-019-0686-2.
- Hugh R Wilson and Jack D Cowan. Excitatory and inhibitory interactions in localized populations of model neurons. *Biophysical journal*, 12(1):1–24, 1972.
- Hao Xu, Alexander Lorbert, Peter J Ramadge, J Swaroop Guntupalli, and James V Haxby. Regularized hyperalignment of multi-set fMRI data. In *2012 IEEE Statistical Signal Processing Workshop (SSP)*, pages 229–232. IEEE, 2012.
- Daniel LK Yamins and James J DiCarlo. Using goal-driven deep learning models to understand sensory cortex. *Nature Neuroscience*, 19(3):356, 2016.